Correlation function analysis of fiber networks: Implications for thermal conductivity

Jorge Martinez-Garcia,[1] Leonid Braginsky,[1,2] Valery Shklover,[1] and John W. Lawson[3]
[1]*Laboratory of Crystallography, Department of Materials, ETH Zurich, CH-8093 Zurich, Switzerland*
[2]*Institute of Semiconductor Physics, RU-630090 Novosibirsk, Russia*
[3]*Thermal Protection Materials Branch, MS 234-1, NASA Ames Research Center, Moffett Field, California 94035, USA*
(Received 27 March 2011; published 17 August 2011)

Transport properties of highly porous fiber structures are investigated. The fibers are assumed to be thin, but long, so that the number of interfiber connections along each fiber is large. We show that the effective conductivity of such structures can be found from the correlation length of the two-point correlation function of the local conductivities. The correlation function in the most interesting cases can be estimated from two-dimensional (2D) images of the structures. This means that the three-dimensional conductivity problem can be considered using 2D digital images of the structure. We apply this approach to analyze the parameters that determine the thermal conductivity of fiber structures.

DOI: 10.1103/PhysRevB.84.054208 PACS number(s): 65.80.−g, 44.30.+v, 68.65.−k, 44.35.+c

I. INTRODUCTION

Composite materials consisting of long fibers with high thermal conductivity (TC) embedded in an amorphous matrix with low thermal conductivity are becoming very common in modern applications. Such materials can be used as thermal barrier coatings. Long fibers are necessary to ensure the mechanical strength of the coating. Long high-TC fibers are also useful to give anisotropic properties to the coating. Ablative thermal protective systems (ATPS) are an example of such materials that are used to protect space vehicles from the extreme environment of atmospheric entry. These materials typically consist of a low density, but rigid, carbon fiber material infiltrated with a phenolic resin.

PICA (phenolic impregnated carbon ablator), a material developed by NASA, is an example of currently used ATPS.[3,4] PICA is made from a carbon fiber insulation (Fiber Materials, Inc. under the trade name Fiberform®) impregnated with a phenolic resin. The typical diameter of the fibers in PICA is 14–16 μm and their length exceeds ∼1600 μm. The resin creates a highly porous thermoset structure after polymerization with a low bulk density ranging from 0.22 to 0.27 g/cm^3. The processing method used for PICA gives a parallel orientation to the fibers, which promotes a low through-the-thickness thermal conductivity, which is an important property for these insulating materials. Characterization of the effective properties of this novel material is a challenging task. Typically, such materials are used at high temperatures when thermal transport occurs through a combination of conduction, radiation, and convection mechanisms. In this paper, however, we concentrate only on the conduction part; the other components will be addressed in future work.

Despite many detailed studies, the full potential of highly porous fibrous materials has not been realized. Further progress will depend on the ability to estimate and model accurately their properties. Sophisticated approaches have been developed to model the thermal response of ATPS. For example, FIAT (Fully Implicit Ablation and Thermal response code) was developed by NASA for one-dimensional (1D) simulation of kinetically controlled pyrolysis, in-depth conduction, blowing due to pyrolysis gases, and surface recession as a function of time using 1D models of ablation for porous materials.[2,5–9] The program TITAN, also developed by NASA, extends FIAT to 2D.[7] However, these programs assume that the materials are homogeneous and therefore do not describe the relationship between microstructure and thermal response.

Direct numerical calculation of transport properties in 3D fiber composites is very difficult (see, e.g., Ref. 10). Indeed, it is often necessary to consider a 3D-transport equation on a fine-structure mesh. The mesh spacing should be much smaller than the fiber thickness, while the total size of the mesh network should exceed the fiber length. Moreover, the composite structure can be very complicated and its microscopic description may require many parameters.[11] The question arises whether all of these parameters are important for TC estimation or whether this estimation can be achieved from knowledge of a smaller set of parameters. We showed previously that knowledge of the two-point correlation function (CF) is sufficient for TC estimation in nonhomogeneous materials of low porosity.[12,13] It is not clear, however, whether the CF is sufficient for modeling the thermal conductivity of highly porous fiber materials (porosity ∼80–90%) or whether higher-order correlation functions will be required.

An important property of fiber structures is their anisotropy. Anisotropy can be created explicitly, however, a typical fiber structure will always be anisotropic due to nematic ordering. The effect of anisotropy on the electrical conductivity in such structures has been studied[14] and exact scaling laws have been obtained.[15] The dependence of TC on fiber orientation was observed, e.g., in oriented fibrous carbon insulation.[2] Room-temperature in-plane thermal conductivity of carbon insulation at 1575 K was reported to be 0.05 W/mK normal to the fibers plane and 0.14 W/mK in the fibers plane. Thermal conductivity of fibrous materials with a phenolic resin matrix was reported to be ∼2.4 higher in the direction of fiber alignment compared to that through-the-thickness.[16] Filled honeycombs, multilayers, and tile-like structures can also be manufactured to yield anisotropic properties of the corresponding structure.[17]

Qualitative estimates of conductivity for fiber structures have been done in Ref. 18. It was shown that the conductivity

can be expressed in terms of the porosity of the structure, the thickness of the fibers, and the mean distance between fiber connections. It is not clear, however, how to estimate these parameters from the two-point correlation function, which is not simple since the CF cannot be approximated with a single exponent or a Gaussian function. This problem will be considered in this paper. We show that the total porosity and the correlation lengths along each (x, y, and z) direction are the only parameters needed to estimate the conductivity of fiber structures.

We start with a simple model of TC, which is a generalization of that proposed in Ref. 18 for anisotropic media. We assume the fibers are long enough, so that each of them has many crossing points along their length. This means also that the number of fibers per unit volume exceeds the percolation threshold. This is the main point that distinguishes our model from the previous studies where only the conductivity near the percolation threshold was investigated.[14] We found that TC can be expressed in terms of the porosity of the structure and the mean distance between the fibers in each direction. In the following two sections, we show that all these parameters can be estimated from the CF.

In Sec. III, we consider 2D models of the structures that consist of straight square fibers with equal thickness and length. For models with different fiber lengths, we can directly measure all parameters of the structure and then compare them to results obtained from the CF calculated from the image of the structure. We relate the parameters of the structure to the correlation lengths of the CF. In Sec. IV, we generalize these results to the 3D case.

II. THERMAL CONDUCTIVITY OF FIBER STRUCTURES

A. Thermal conductivity of the Fiberform

Fiberform is the starting material for PICA, which is composed exclusively of fibers before infiltration with the resin. At low temperatures, heat conduction through the fiber network is the primary mechanism of thermal transport in such structures. We assume Fiberform to be an array of cylindrically shaped fibers, each fiber being geometrically characterized by its length l and diameter d. If n is the fiber concentration, i.e., the number of fibers in the unit cube, then these three parameters: l, d, and n, will characterize Fiberform. We introduce also the fiber density as $V_f = \pi n d^2 l/4$ ($V_f = ndl$ in the 2D case). All fibers will intersect in a 2D model, if they are long enough and close. This is not the case in 3D models, since noncoplanar fibers can be skewed.

We assume that the fibers are thin ($d \ll l$) and long, so that the mean distance between neighboring connecting points λ is small compared to the fiber length ($\lambda \ll l$). This also means that the concentration of fibers is large enough, so that we are well above the percolation threshold.

Suppose an external thermal gradient is applied along the z axis, and assume cylindrical symmetry for the fiber network with respect to this axis, i.e., we consider heat flow along the z direction (see Fig. 1). We consider two points on the fibers in the plane $z = \text{const}$. The temperature T at these

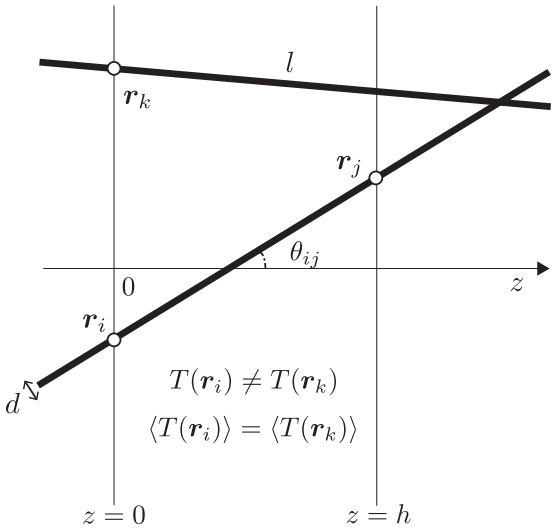

FIG. 1. Schematic of heat transport in a fiber structure. Axis z is the direction of heat flux.

points can be different but their average values are equal. Indeed, the condition $\lambda \ll l$ means the existence of percolation between the points, while $\langle T(\boldsymbol{r}_i)\rangle \neq \langle T(\boldsymbol{r}_k)\rangle$ ensures a heat flux between them. The latter is forbidden by cylindrical symmetry, therefore $\langle T(\boldsymbol{r}_i)\rangle = \langle T(\boldsymbol{r}_k)\rangle$.

Let us find the heat flux I_{ij} through a fiber connecting two points $\boldsymbol{r}_i$ and $\boldsymbol{r}_j$ at two close planes $z = 0$ and $z = h$, respectively (see Fig. 1):

$$I_{ij} = \frac{\pi \kappa_f d^2}{4 l_{ij}} [T(\boldsymbol{r}_i) - T(\boldsymbol{r}_j)].$$

Here, κ_f is the fiber thermal conductivity, $l_{ij} = |\boldsymbol{r}_i - \boldsymbol{r}_j| = h/|\cos\theta_{ij}|$, and θ_{ij} is the angle between the fiber and the z axis. The total flux through the plane $z = 0$ is equal to the sum of all the fluxes over all fibers crossing the plane:

$$\Phi = \sum I_{ij} = \frac{\kappa_{\text{eff}} S}{h} [\langle T(\boldsymbol{r}_i)\rangle - \langle T(\boldsymbol{r}_j)\rangle].$$

This allows us to determine the effective thermal conductivity κ_{eff} as

$$\kappa_{\text{eff}} = \frac{\pi \kappa_f d^2 N}{4S[\langle T(\boldsymbol{r}_i)\rangle - \langle T(\boldsymbol{r}_j)\rangle]} \langle \cos\theta_{ij} [T(\boldsymbol{r}_i) - T(\boldsymbol{r}_j)]\rangle.$$

Here, $N = 4S/\pi D_\perp^2$ is the total number of fibers crossing the plane $z = 0$, S is the side area of the specimen in this plane, and $D_\perp$ is an average distance between the fibers crossing the plane $z = 0$. Assuming that $\langle \cos\theta_{ij}[T(\boldsymbol{r}_i) - T(\boldsymbol{r}_j)]\rangle = \langle \cos\theta_{ij}\rangle \langle [T(\boldsymbol{r}_i) - T(\boldsymbol{r}_j)]\rangle$, one finds

$$\kappa_{\text{eff}} = \frac{d^2}{D_\perp^2} \kappa_f \quad \text{or} \quad \kappa_{\text{eff}} = \frac{D_\parallel}{D_\parallel + 2D_\perp} V_f \kappa_f, \tag{1}$$

where $D_\parallel$ is an average distance between the fibers along the z direction, so that $V_f = d^2(D_\parallel + 2D_\perp)/(D_\perp^2 D_\parallel)$.

In a similar way, we can consider TC across the z axis. The results are

$$\kappa_{\parallel} = \frac{d^2}{D_{\perp}^2}\kappa_f, \quad \kappa_{\perp} = \frac{d^2}{D_{\parallel}D_{\perp}}\kappa_f,$$

or equivalently,

$$\kappa_{\parallel} = \frac{D_{\parallel}}{D_{\parallel}+2D_{\perp}}V_f\kappa_f, \quad \kappa_{\perp} = \frac{D_{\perp}}{D_{\parallel}+2D_{\perp}}V_f\kappa_f, \qquad (2)$$

where $\kappa_{\parallel}$ and $\kappa_{\perp}$ are the components of the effective TC along and across the z axis, respectively. Thus

$$\begin{aligned} 2\kappa_{\perp}+\kappa_{\parallel} &= V_f\kappa_f, \\ \kappa_{\perp}/\kappa_{\parallel} &= D_{\perp}/D_{\parallel}. \end{aligned} \qquad (3)$$

The former equality represents the trace of the conductivity tensor, which is invariant with respect to the axis used. The latter equality is in agreement with Ref. 15. In particular, for an isotropic structure $D_{\parallel} = D_{\perp} = D$, the effective TC becomes

$$\kappa_{\text{eff}} = \frac{d^2}{D^2}\kappa_f = \frac{1}{3}V_f\kappa_f.$$

The factor $1/3$ appearing in the last equation indicates that the rule of mixtures cannot be applied to the fiber structures. To understand the reason, let us consider TC along the side of a simple cubic fiber network. We assume thin fibers, so that heat propagation exists only along the fibers, but not across them. Therefore, only fibers oriented along the applied temperature gradient participate in TC. The effect of the other $2/3$ fibers can be estimated, if we replace the cube side D by $D-d$. Then $\kappa_{\text{eff}} = d^2/(D-d)^2 \approx (1+2d/D)d^2/D^2$. The factor $1/3$ disappears when $d \simeq D$.

B. Thermal conductivity of ATPS

In this section, we consider a material consisting of fibers embedded in a matrix with small TC, $\kappa_M \ll \kappa_f$. The effect of the matrix is twofold. First, there can be a direct heat flux across the matrix. Second, there can be heat transport through the fibers and across narrow bridges between two skewed fibers. The second effect can be important, if the thermal resistivity of such bridges is on the order of the resistivity of the fibers between two connection points. Let us first consider the second effect.

Let δ be the length of such a bridge. The bridge is important if its resistivity is less than or comparable to the resistivity of the appropriate fiber part, i.e., $\delta/\kappa_M \lesssim \lambda^*/\kappa_f$. Here, λ^* is the distance between two bridges whose size is less than δ. It can be estimated similarly to Eq. (9):

$$\lambda^* = \frac{3}{2n(d+\delta/2)l}.$$

Considering the cube, $\lambda^*\times\lambda^*\times\lambda^*$, we can write its resistivity as

$$R = \left(\frac{\lambda^*}{\kappa_f d^2} + \frac{\delta}{\kappa_M d^2}\right)\frac{D^2}{\lambda^{*2}} = \frac{1}{\lambda^*\kappa_{\text{eff}}},$$

from which one finds

$$\kappa_{\text{eff}} = \frac{\lambda^* d^2/D^2}{\lambda^*/\kappa_f + \delta/\kappa_M} = \frac{d^2/D^2}{1/\kappa_f + \delta/\lambda^*\kappa_M}. \qquad (4)$$

The above relation coincides with a similar estimation for κ_{eff} in Ref. 18, if we assume, $\delta/\lambda^* = d^2/\lambda^2$ or $\delta \simeq V_f d$. Equation (4) turns into Eq. (1), if the last term in its denominator is omitted. This is possible when $\delta/\lambda^* \ll \kappa_M/\kappa_f$ or $V_f\delta^2/d^2 \ll \kappa_M/\kappa_f$.

Another way to take the bridges into account consists of assuming each fiber is surrounded by some layer, so that the thickness of each fiber is $\delta_0 > d$ and its effective TC is $\tilde{\kappa} = [\kappa_f d^2 + \kappa_M(\delta_0^2 - d^2)]/\delta_0^2$. Substituting the latter into Eq. (1) with $d \to \delta_0$ yields

$$\kappa_{\text{eff}} = \frac{\kappa_f d^2 + \kappa_M\left(\delta_0^2 - d^2\right)}{D^2}.$$

This means that the fiber network and the matrix can be considered as two resistors connected in parallel. Therefore, the TC of the structure can be estimated as[19]

$$\kappa_{\text{eff}} = \frac{1}{3}V_f\kappa_f + \left(1 - \frac{4}{3}V_f\right)\kappa_M. \qquad (5)$$

III. CORRELATION FUNCTION OF THE 2D FIBER STRUCTURES

In order to estimate the parameters $D_{\parallel}$ and $D_{\perp}$ required for TC modeling, we consider the CF of fiber structures. We introduce the CF as

$$W(\boldsymbol{r},\boldsymbol{r}') = \frac{\langle[\eta(\boldsymbol{r}) - \langle\eta(\boldsymbol{r})\rangle][\eta(\boldsymbol{r}') - \langle\eta(\boldsymbol{r}')\rangle]\rangle}{4V_f(1-V_f)}, \qquad (6)$$

where $\langle\cdots\rangle$ denotes an ensemble average and the characteristic function $\eta(\boldsymbol{r})$ is given by

$$\eta(\boldsymbol{r}) = \begin{cases} 1, & \text{if } \boldsymbol{r} \text{ is inside a fiber,} \\ -1, & \text{otherwise.} \end{cases}$$

For statistically homogeneous media, Eq. (6) depends only on the difference between two arbitrary points $\boldsymbol{r}$ and $\boldsymbol{r}'$, $[W(\boldsymbol{r},\boldsymbol{r}') = W(\boldsymbol{r}-\boldsymbol{r}')]$; it is equal to unity at the coordinates origin, $W(0) = 1$ and vanishes at infinity. If the media is isotropic, then $W(\boldsymbol{r},\boldsymbol{r}') = W(|\boldsymbol{r}-\boldsymbol{r}'|)$. The aim of this section is to calculate the CF using the structure image and to estimate the parameters of the structure from the appropriate correlation lengths. We will see that the CF is determined by the fiber thickness d and the distance between the intercrossing points of the fibers, if their density is large enough. Otherwise, the fiber length becomes the second correlation length. To evaluate the CF from digital images, we employed the procedure outlined in Ref. 20.

Figure 2 displays the 2D fiber models and the corresponding CF. All the structures are composed of similar fibers; they have the same positions and orientations, and are distinguished by the fiber length only. Fibers in Fig. 2 (a) are short, so that they do not intersect. The corresponding CF have two correlation lengths: one of them is related to the fiber thickness ($r/d = 1$) and the other one to the fiber length. The CF of different structures of this figure are well distinguished.

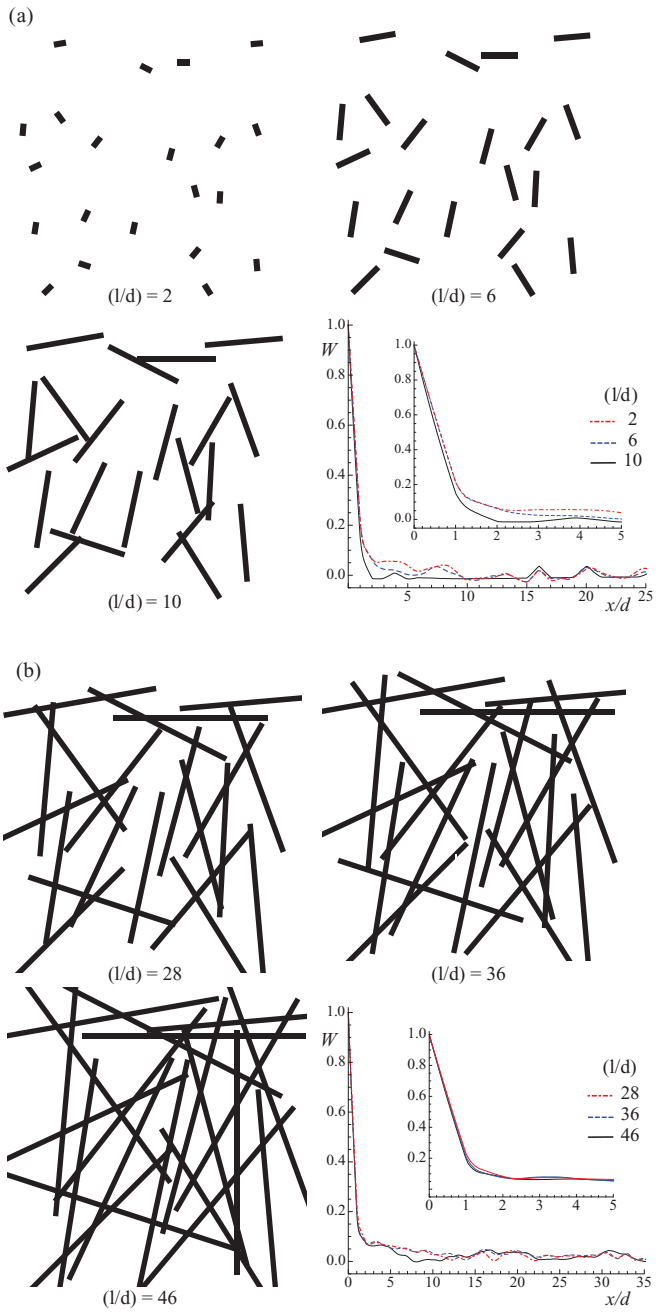

FIG. 2. (Color online) Two-dimensional models of fiber structures and corresponding correlation functions W taken along the horizontal axis x. (a) Short-fiber models with aspect ratio, $(l/d) = 2$,6, and 10 and $V_f = 0.01$, 0.04, and 0.07, respectively. (b) Long-fiber models with aspect ratio, $(l/d) = 28$, 36, and 46 and $V_f = 0.17$, 0.21, and 0.26, respectively. All fibers have the same positions, orientations, and thickness in each model. A thickness value of $d = 0.5$ unit was used in the computations.

On the contrary, the CF in Fig. 2(b) are very similar. This is because the second correlation length for long fibers is the mean distance between the intercrossing points, but not the fiber length. Direct calculation of this distance (from the image using, e.g., Photoshop software) yields about $9d$ for all of the structures in Fig. 2(b).

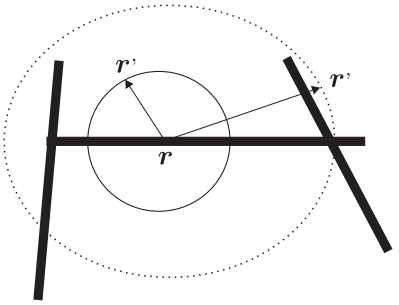

FIG. 3. Long fibers. Small circle intersects the fiber two times (bold line). Large circle has many points of intersection (dashed line).

In order to understand the difference between the CF behavior in Figs. 2(a) and. 2(b), let us consider the two-point probability function[21,22]

$$S = \langle \eta_0(\boldsymbol{r})\eta_0(\boldsymbol{r}')\rangle, \tag{7}$$

where

$$\eta_0(\boldsymbol{r}) = \begin{cases} 1, & \text{if } \boldsymbol{r} \text{ is inside a fiber,} \\ 0, & \text{otherwise.} \end{cases}$$

Then $S = V_f$, if $|\boldsymbol{r} - \boldsymbol{r}'| \ll d$, i.e., if both $\boldsymbol{r}$ and $\boldsymbol{r}'$ are either inside or outside the fiber. In order to estimate S for a longer distance, $|\boldsymbol{r} - \boldsymbol{r}'| \gg d$, we have to multiply the probability that the point $\boldsymbol{r}$ belongs to the fiber $[P(\boldsymbol{r} \in \text{fiber}) = V_f]$ by the probability that the point $\boldsymbol{r}'$ belongs to the fiber $[P(\boldsymbol{r}' \in \text{fiber})]$ provided that the first point $\boldsymbol{r}$ is on the fiber. The latter probability can be easily estimated, if we assume an isotropic fiber structure and draw a circle around $\boldsymbol{r}$, as shown in Fig. 3. Then $P(\boldsymbol{r}' \in \text{fiber})$ can be estimated as the ratio of the fiber thickness inside the circle to the circle length. For short fibers [see Fig. 2(a)], $P(\boldsymbol{r}' \in \text{fiber}) = d/\pi|\boldsymbol{r} - \boldsymbol{r}'|$, if $d \ll |\boldsymbol{r} - \boldsymbol{r}'| \ll l$, and $P(\boldsymbol{r}' \in \text{fiber}) = V_f$, if $|\boldsymbol{r} - \boldsymbol{r}'| \gg l$; in the latter case, both probabilities are independent. For long fibers [see Fig. 2(b)], $P(\boldsymbol{r}' \in \text{fiber}) = d/\pi|\boldsymbol{r} - \boldsymbol{r}'|$, if $d \ll |\boldsymbol{r} - \boldsymbol{r}'| \ll l_c$, where l_c is the mean distance between the crossing points. Note that $P(\boldsymbol{r}' \in \text{fiber})$ increases, when $|\boldsymbol{r} - \boldsymbol{r}'| > l_c$. Such an increase can be found in the CF of Fig. 2(b) at $|\boldsymbol{r} - \boldsymbol{r}'| \approx 10d$. For $|\boldsymbol{r} - \boldsymbol{r}'| \gg l_c$, $S = V_f^2$ since $P(\boldsymbol{r} \in \text{fiber})$ and $P(\boldsymbol{r}' \in \text{fiber})$ are independent at the large distances. From the above, Eq. (7) can be rewritten as

$$S = \begin{cases} V_f, & |\boldsymbol{r} - \boldsymbol{r}'| \ll d, \\ \dfrac{d}{\pi|\boldsymbol{r} - \boldsymbol{r}'|}, & d \ll |\boldsymbol{r} - \boldsymbol{r}'| \ll l_c, \\ V_f^2, & |\boldsymbol{r} - \boldsymbol{r}'| \gg l_c. \end{cases}$$

Since $\eta(r) = 2\eta_0(r) - 1$, it follows from Eqs. (6) and (7) that

$$W(\boldsymbol{r} - \boldsymbol{r}') = \frac{S(\boldsymbol{r} - \boldsymbol{r}') - V_f^2}{V_f(1 - V_f)},$$

thus

$$W(\boldsymbol{r}-\boldsymbol{r}') = \begin{cases} 1, & |\boldsymbol{r}-\boldsymbol{r}'| \ll d, \\ \dfrac{d}{\pi\,|\boldsymbol{r}-\boldsymbol{r}'|\,(1-V_f)} - \dfrac{V_f}{1-V_f}, & d \ll |\boldsymbol{r}-\boldsymbol{r}'| \ll l_c, \\ 0, & |\boldsymbol{r}-\boldsymbol{r}'| \gg l_c. \end{cases} \tag{8}$$

A similar behavior of CF was found in Fig. 2(b). Note that $d/|\boldsymbol{r}-\boldsymbol{r}'| \gg V_f$ if $|\boldsymbol{r}-\boldsymbol{r}'| \ll l_c$.

Apparently, it is the connectivity (λ), i.e., the mean distance between crossing points, not the mean length of the fibers that determines the transport properties in the fiber structure. We have shown that the connectivity coincides with the correlation length of the CF in the 2D case, $\lambda \simeq l_c$. Therefore, it can be estimated from Eq. (6). It is the connectivity, which determines the conduction pathways. They are roughly the same in the Fig. 2(b), thus all these structures have the same TC. Lengthening of the fibers in this case means an increase of dead ends, but it does not change the conductivity. An increase in TC can be expected when fibers becomes so long that the number of crossing points increases. Thus the connectivity value decreases and therefore the conductivity increases.

IV. CORRELATION FUNCTION OF THE 3D FIBER STRUCTURES

The main difference between 2D and 3D models concerns the intersection of the fibers. Indeed, the fibers in the 2D model intersect, if they are long enough and close. In general, fibers in the 3D structure can be skewed; this happens with fibers that are not coplanar. If so, the mean distance between crossing points will exceed the distance between the fibers. The question arises what is the second correlation length discussed in the previous section? Is it related to the connectivity or to the mean distance between the fibers?

Let us first estimate the connectivity λ. Consider a large parallelepiped, $L \times L \times \lambda$ ($L \to \infty$). The number of fibers inside the parallelepiped is $N = nL^2\lambda$, and their total projection on the $L \times L$ plane is $(2/3dl)N$. This projection should cover the entire plane, if λ is the distance between crossing points. Thus

$$\lambda = \frac{3}{2ndl}. \tag{9}$$

The mean distance between the fibers D, can be estimated as $D^2nl = 1$ or

$$D = \frac{1}{\sqrt{nl}}.$$

Then for the ratio λ/D, we obtain

$$\frac{\lambda}{D} = \frac{3}{4}\sqrt{\frac{\pi}{V_f}} \approx \frac{1}{\sqrt{V_f}},$$

where $V_f = \pi nd^2l/4$ is the density of the 3D fiber structure. This value is not so large for $V_f \simeq 0.1$.

It is interesting to compare λ with the fiber length l:

$$\frac{\lambda}{l} = \frac{3}{2ndl^2}.$$

From this relation, it is evident that $\lambda \sim l$, if $ndl^2 \sim 1$, i.e., the fiber concentration $n_c = (dl^2)^{-1}$ determines the percolation threshold. Indeed, at $n = n_c$, we have only one fiber in the $l \times l \times d$ box. The fibers are not connected if $n \ll n_c$, but connected in the opposite limit. The mean number of connections per fiber is $l/D \sim l\sqrt{ln}$. In this paper, we assume this value to be large.

For a rough estimation of the correlation function in 3D we have to replace the circle in Fig. 3 with a sphere, so that the conditional probability $P(\boldsymbol{r}' \in \text{fiber})$ provided by the first point $\boldsymbol{r}$ is in the fiber is now $P(\boldsymbol{r}' \in \text{fiber}) = d^2/8\,|\boldsymbol{r}-\boldsymbol{r}'|^2$. Therefore, Eq. (8) becomes

$$W(\boldsymbol{r}-\boldsymbol{r}') = \begin{cases} 1, & |\boldsymbol{r}-\boldsymbol{r}'| \ll d, \\ \dfrac{d^2}{8\,|\boldsymbol{r}-\boldsymbol{r}'|^2\,(1-V_f)} - \dfrac{V_f}{1-V_f}, & d \ll |\boldsymbol{r}-\boldsymbol{r}'| \ll D, \\ 0, & |\boldsymbol{r}-\boldsymbol{r}'| \gg D. \end{cases} \tag{10}$$

For the correlation length we obtain thus $l_c \simeq D$.

For the purpose of illustrating how the 3D case can be treated, we have simulated 3D fiber structures and extracted cross-section images from them (see Fig. 4). The algorithm employed to produce such structures allows free intercrossing of the fibers, so that nematic ordering does not occur. It relies on the basic ideas discussed by Berryman,[20] but it has been modified for cylindrical geometry in this work. Figures 4(b) and 4(c) display one such cross section ($z = 15$) and the corresponding $W(x,0)$ and $W(0,y)$ of a fully random fiber structure. As it can be appreciated, these functions are very close because both the x and the y directions are equal. The CF allows estimation of the mean distance among fibers as $D = 2d$. This does not occur when the fibers have a preferred

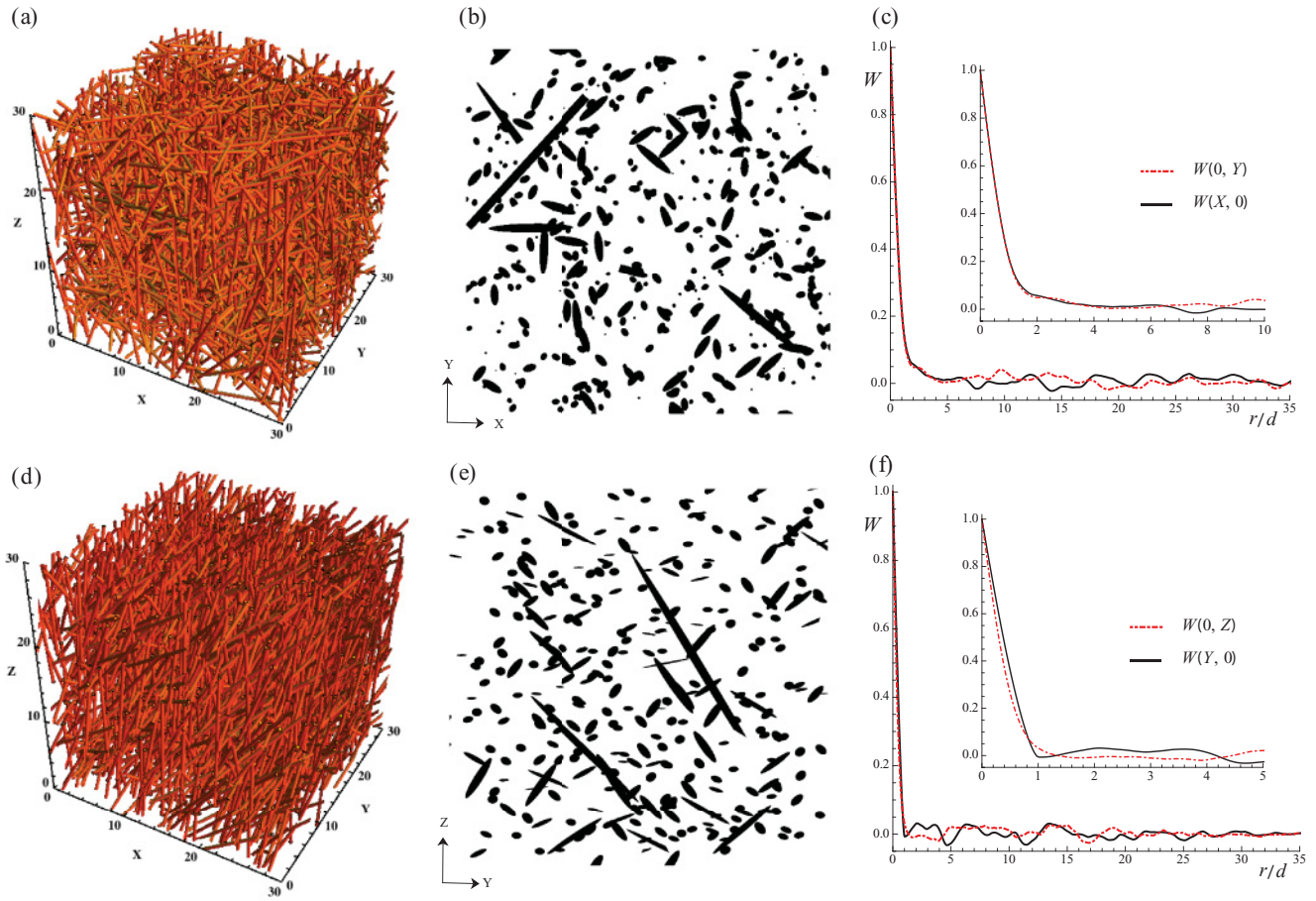

FIG. 4. (Color online) Cross section images and corresponding correlation functions of 3D models of fiber structures. (a) Fibers randomly positioned and oriented in space. (b) Cross-section image of (a) at $z = 15$. (c) Correlation functions $W(x,0)$ and $W(0,y)$ of (b) taken along the x and y axes, respectively. (d) Fibers randomly positioned with preferred orientation along the z axis. (e) Cross-section image of (d) at $x = 10$. (f) Correlation functions of (e) taken along the y and z axes. A total number of $N = 2000$ cylindrically shaped fibers with aspect ratio $(l/d) = 40$ and $V_f = 0.21$ were considered in the simulations.

orientation [see Fig. 4(d)] and we consider a cross section containing the preferred axis [see Fig. 4(e)]. The CF measured along the preferred axis and along the direction perpendicular to it display different correlation lengths as shown in Fig. 4(f).

It is interesting to consider the Fourier transform of the correlation function. For the simple CF given in Eq. (10) and $d \ll D$, it has the form

$$\tilde{W}(k) = \frac{4\pi V_f}{(1 - V_f)k^3}[\sin(kD) - kD\cos(kD)]. \qquad (11)$$

In Eq. (11), we omit small values, which oscillate as $\cos(kd)$. Thus we can estimate the value of D by analyzing the oscillations of the Fourier transform of the CF. This is important for correlation functions measured from structure images.

Figure 5 shows the cross section of the 3D Fiberform scanned with a novel high contrast microtomography system, Model MicroXCT (Xradia Inc, Pleasanton), its correlated function, and the Fourier transform. It is not easy to estimate the correlation length directly from the CF because of noise [see Fig. 5(b)]. However, it can be estimated from the Fourier transform since the period of the shortest oscillations is equal to $2\pi/D$. For an anisotropic structure, such as that shown in Fig. 5(a), this criterion allows the estimation of the ratio $D_\perp/D_\parallel$, which determines the anisotropy of the thermal conductivity along and across the structure axes.

Let us estimate the thermal conductivity of the Fiberform presented in Fig. 5. The volume fraction of the fibers can be calculated directly from the digital image of Fig. 5(a); we found it equal to $V_f = 0.1$. The diameter of the fibers corresponds to the first correlation length of CF; we found $d \approx 15\,\mu$m from Fig. 5(b). If we assume a fiber length of $l = 1600\,\mu$m, then for the fiber concentration $n = 4V_f/\pi d^2 l$, we find $n \approx 3.5 \times 10^5 \text{cm}^{-3}$. This value exceeds the percolation threshold $n_c = 1/dl^2 \approx 2.6 \times 10^4\,\text{cm}^{-3}$. Rough estimation of the mean distance between the fiber connections gives $\lambda = 3/2ndl \approx 180\,\mu$m; so that there are about $l/\lambda \approx 10$ connections for each fiber. Thus all assumptions previously made to estimate the heat transport are satisfied. The distances between two adjacent peaks in both, bold and dashed, curves in Fig. 5(c) are equal to $0.045\,\mu\text{m}^{-1}$. This means that $D_\parallel = D_\perp \approx 140\,\mu$m. This estimate can be observed in Fig. 5(b) as well. Then Eq. (3) yields $\kappa_\parallel = \kappa_\perp \approx 0.03\kappa_f$.

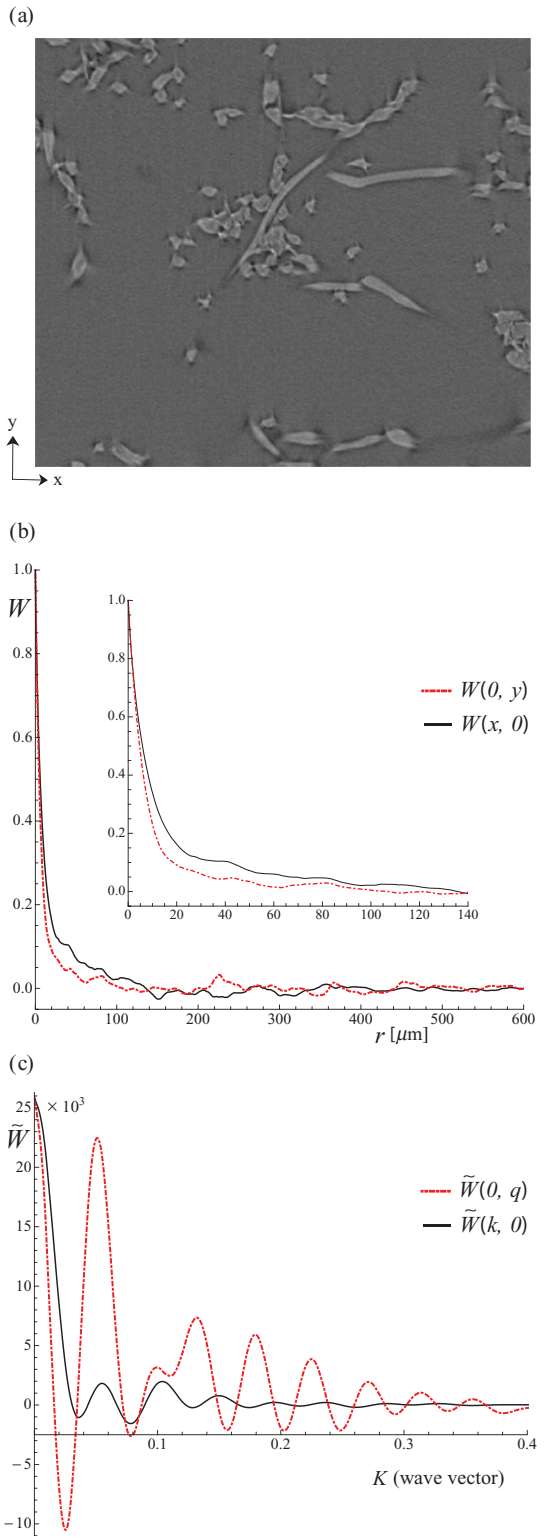

FIG. 5. (Color online) (a) MicroXCT scanned at 0.5 micron voxelCross section of 3D Fiberform from, (b) its correlation function W and (c) Fourier transform of W in x and y directions. [Image (a) provided to NASA courtesy of Xradia, Inc.]

V. DISCUSSION

We found that the inequality $n \gg n_c$ holds well for the structure in Fig. 5. The same estimation can be done also for the ablative thermal protection structure[1] mentioned in the introduction. Note also that the percolation threshold $V_{fc} = \pi d^2 l n_c/4$, which was estimated in Ref. 14 for $l/d = 80$, yields $V_{fc} = 0.03$, while a typical volume concentration for the fibers in such structures is $V_f = 0.1$–0.2. This means that Eq. (3) can be used for TC estimation, and the result is in agreement with experiments.[2,16]

More interesting is the effect of anisotropy. In Sec. II, we found the simple estimation (2), which depends on the correlation lengths $D_\parallel$ and $D_\perp$, but is independent of the connectivity λ. This result seems surprising, but it can be understood from the following example. Let us consider the thermal conductivity of a cubic mesh of fibers. It can be estimated as the thermal conductivity of the $\lambda \times \lambda \times \lambda$ cube. The number of disconnected fibers within the cube is $(\lambda/D)^2$ and the resistivity of each fiber is $4\lambda/\pi d^2 \kappa_f$. The resistivity of the cube can then be written as $(4\lambda/\pi d^2 \kappa_f)(\pi D^2/4\lambda^2)$ or $1/\lambda\kappa_{\text{eff}}$. Thus

$$\kappa_{\text{eff}} = \left(\frac{d}{D}\right)^2 \kappa_f .$$

This result will not change if we had disconnected some of the contacts in the cubic mesh. The result changes only if we disconnect all the contacts along the fibers. Therefore, the error of the estimation (3) cannot be better than $\lambda/l \sim n_c/n$. This is the effect of dead ends, which is not important far from the percolation threshold n_c. For the same reason, small bridges of matrix material do not affect the thermal conductivity in the case of a fiber-matrix composite.

Another reason for the error in Eq. (3) comes from the dispersion of the resistivity of fiber segments between two contacts. This effect can be estimated with the factor[23]

$$\Phi = \left(1 + \frac{2\sigma^2}{N}\right)^{-1},$$

where σ is the relative dispersion of the resistivity (i.e., relative dispersion of the length between adjacent contacts in our case) and $N \geqslant 6$ in the 3D resistor net. Assuming $\sigma \lesssim 0.5$, we estimate the relative error as 0.1.

Typically, the matrix material (phenolic resin) can be porous itself. The size of these pores is very small, and their effect can be estimated if we make the substitution[19] $\kappa_M \to \kappa_M(1 - \frac{4}{3} p_M)$, where p_M is the intrinsic matrix porosity. This makes the effect of the matrix negligible.

Estimation of the conductivity of anisotropic structures can be performed using Eq. (3). Indeed, the fiber density V_f can be obtained from the structure porosity, while the ratio of the correlation lengths, $D_\perp/D_\parallel$, can be estimated by analyzing the oscillations of the Fourier transforms of the CF across and along the structure [see Fig. 5(b)].

We calculated the correlation function of model structures. The same calculation can be made also using SEM or optical images of cross sections. Similar images can also be obtained from X-ray tomography [see Fig. 5(a)]. Basically one slice is enough for the CF calculation; however, its accuracy can be significantly increased if we use several slices and average the results.

In conclusion, we have analyzed expressions (2) for the thermal conductivity of fiber structures and have investigated the estimation of its parameters from information provided by the CF analysis.

ACKNOWLEDGMENT

This work was supported by the Swiss National Science Foundation (Grant 200021 − 130274/1).

[1]M. Stackpole, S. Sepka, I. Cozmuta, and D. Kontinos, *Post-flight Evaluation of Stardust Sample Return Capsule Forebody Heatshield Material*, 46th AIAA Aerospace Sciences Meeting and Exhibit, Orlando, Florida, January 2008, AIAA Paper 2008-1202 (2008).

[2]T. G. Godfrey, D. L. McElroy, and Z. L. Ardary, Nucl. Technol. **22**, 94 (1974).

[3]H. Tran, C. E. Johnson, D. J. Rasky, F. C. Hui, M.-T. Hsu, T. Chen, Y.-K. Chen, D. Paragas, and L. Kobayashi, *Phenolic Impregnated Carbon Ablators (PICA) as Thermal Protection Systems for Discovery Missions*, NASA TM-110440 (1997).

[4]M. A. Covington, J. M. Heineman, H. E. Goldstein, Y.-K. Chen, Terrazas-Salinas, J. A. Balboni, J. Olejniczak, and E. R. Martinez, J. Spacecr. Rockets **45**, 854 (2008).

[5]Y.-K. Chen and Frank S. Milos, J. Spacecr. Rockets **36**, 475 (1999).

[6]M. A. Covington, J. M. Heinemann, H. E. Goldstein, Y.-K. Chen, I. Terrazas-Salinas, J. A. Balboni, J. Olejniczak, and E. R. Martinez, *Performance of a Low-Density Ablative Heat Shield Material*, 37th AIAA Thermophysics Conference, June 2004, AIAA Paper 2004-2273 (2004).

[7]Y.-K. Chen and W. D. Henline, AIAA Paper 93-027 (1993).

[8]*Users Manual* (MARC Analysis Research Corp., Palo Alto, CA, 1994), Vol. **A**, p. E5.0.1-A1.8.

[9]T. H. Squire, F. S. Milos, G. C. Hartlieb, and D. J. Rasky, *TPSX: Thermal Protection System Expert and Material Property Database*, Proceedings of Fourth International Conference on Composite Engineering, edited by D. Hui (International Community for Composites Engineering and College of Engineering, Univ. of New Orleans, LA, 1997), p. 937.

[10]O. Coindreau and G. L. Vignoles, J. Mater. Res. **20**, 2328 (2005).

[11]G. L. Vignoles, O. Coindreau, A. Ahamadi, and D. Bernard, J. Mater. Res. **22**, 1537 (2007).

[12]L. Braginsky, V. Shklover, G. Witz, and H.-P. Bossmann, Phys. Rev. B **75**, 094301 (2007).

[13]L. Braginsky and V. Shklover, Phys. Rev. B **78**, 224205 (2008).

[14]S. I. White, B. A. DiDonna, M. Mu, T. C. Lubensky, and K. I. Winey, Phys. Rev. B **79**, 024301 (2009).

[15]X. Zheng, M. G. Forest, R. Lipton, R. Zhou, and Q. Wang, Adv. Funct. Mater. **15**, 627 (2005).

[16]M. Moniruzzamann and K. I. Winey, Macromolecules **39**, 5194 (2006).

[17]F. S. Milos and Y.-K. Chen, *Two-Dimensional Ablation, Thermal Response, and Sizing Program for Pyrolyzing Ablators*, 49th AIAA Aerospace Sciences Meeting and Exhibit, Orlando, Florida, January 2008, AAIA Paper 2008-1223 (2008).

[18]T. Hu, A. Yu. Grosberg, and B. I. Shklovskii, Phys. Rev. B , **73**, 155434 (2006).

[19]P. G. Klemens, High Temp. High Press. **23**, 241 (1991).

[20]J. G. Berryman, J. Appl. Phys. **57**, 2374 (1985).

[21]S. Torquato, *Random Heterogeneous Materials: Microstructure and Macroscopic properties* (Springer-Verlag, New York, 2002).

[22]M. Sahimi, *Heterogeneous Materials* I. *Linear Transport and Optical Properties* (Springer-Verlag, New York, 2003).

[23]L. Braginsky, N. Lukzen, V. Shklover, and H. Hofmann, Phys. Rev. B **66**, 134203 (2002).